

GLOBAL HYDROLOGY

Satellites reveal widespread decline in global lake water storage

Fangfang Yao^{1*}, Ben Livneh^{1,2}, Balaji Rajagopalan^{1,2}, Jida Wang³, Jean-François Crétaux⁴, Yoshihide Wada^{5,6}, Muriel Berge-Nguyen⁴

Climate change and human activities increasingly threaten lakes that store 87% of Earth's liquid surface fresh water. Yet, recent trends and drivers of lake volume change remain largely unknown globally. Here, we analyze the 1972 largest global lakes using three decades of satellite observations, climate data, and hydrologic models, finding statistically significant storage declines for 53% of these water bodies over the period 1992–2020. The net volume loss in natural lakes is largely attributable to climate warming, increasing evaporative demand, and human water consumption, whereas sedimentation dominates storage losses in reservoirs. We estimate that roughly one-quarter of the world's population resides in a basin of a drying lake, underscoring the necessity of incorporating climate change and sedimentation impacts into sustainable water resources management.

Lakes cover 3% of the global land area (1), storing standing or slowly flowing water that provides essential ecosystem services of fresh water and food supply, waterbird habitat, cycling of pollutants and nutrients, and recreational services (2). Lakes are also key components of biogeochemical processes and regulate climate through cycling of carbon (3). The potential goods and services from lakes are modulated by lake water storage (LWS) (4), which fluctuates in response to changes in precipitation and river discharge, as well as in response to direct human activities (damming and water consumption) and climate change (5–7). It is well documented that some of the world's largest lakes have recently experienced a decline in water storage (4, 6–9). However, the drivers of LWS decline have either been poorly constrained by inconsistent methods and assumptions or remain unknown for the majority of unstudied large lakes ($>100 \text{ km}^2$) that lack a decadal-scale LWS record (10). For example, recent level declines in the Caspian Sea have been primarily attributed to entirely different processes, either evaporative losses from the water body (11) or decreasing river discharge (12). Similarly, the recent decadal decline of China's largest freshwater body,

Lake Poyang, has been separately attributed to either the operation of the Three Gorges Dam (9) or climate variability (13). More broadly, there have been indications of global shifts in LWS over recent decades. Between 1984 and 2015, a loss of $90,000 \text{ km}^2$ of permanent water area was observed by satellites—an area equivalent to the surface of Lake Superior, whereas $184,000 \text{ km}^2$ of new water bodies, primarily reservoirs, were formed elsewhere (14). Yet, trends and drivers of global LWS remain poorly known, which impedes sustainable management of surface water resources, both now and in the future.

The estimation of trends and variability in global LWS has been complicated by modeling and observational limitations. Current global hydrologic models either neglect LWS changes (15) or provide oversimplified simulations using one-dimensional models of lake volume changes (16). In situ measurements of lakes are spatially sparse, have irregular temporal coverage, or are generally in decline (17). Satellites provide a crucial dimension for assessing large-scale LWS variability through repeated observations of lake areas and water levels from space. However, sensor limitations, such as coarse resolution, infrequent overpasses, large inter-track spacing, and mission gaps, prevent the direct development of a global inventory of LWS changes over time. As a result, existing global-scale studies that document lake volume changes lack the capability to attribute decadal-scale LWS variability because of limited spatial coverage (10, 18, 19), short temporal duration (<2 years) (20), or large gaps in the LWS time series (>9 years) (21). Using NASA's ICESat-2 satellite and a one-dimensional model (assuming a constant lake area), a recent study mapped water levels and storages in 227,386 global water bodies over 2018–2020 and found that reservoirs, defined as water bodies regulated by a dam, dominated seasonal variability in global lake water storage

(20). Given the brevity of the study period (<2 years) and limited attribution, i.e., only separating natural lakes and reservoirs (20), decadal-scale LWS variability and attribution remain an open question. Another study combined water levels from ICESat and ICESat-2 to map LWS changes in 6567 lakes over 2003–2020 and compared LWS changes across different climate regimes (21) but suffered from a 9-year discontinuity (2010–2018) in LWS time series and limited ability to capture and diagnose drivers of interannual variability and trends over the recent decades. Therefore, the human and climate change footprints on global LWS changes over decadal timescales remain critically unknown.

To address this challenge, we construct a global database of time-varying LWS (GLWS) from 1992 to 2020, and then decouple the impacts of anthropogenic and natural factors on decadal-scale variability in LWS (Fig. 1). This GLWS archive consists of subyearly storage time series for 1972 large water bodies, including 1051 natural lakes (100 to $377,002 \text{ km}^2$) and 921 reservoirs (4 to $67,166 \text{ km}^2$), which account for 96 and 83% of Earth's natural lake and reservoir storage, respectively (1, 22). We focus on large lakes because of the fidelity of satellite observations at this scale and their dominance in controlling total lake volume change (8, 20), as well as their importance for human and wildlife populations (23). We leverage recent advances in both algorithms (24) and cloud-based parallel computing to construct time-varying water areas for these lakes using a total of 248,649 Landsat satellite images at a 30-m resolution (materials and methods). We estimate lake volume variability by combining water areas with water surface elevation measurements from satellite altimeters, including CryoSat-2, ENVISAT, ICESat, ICE-Sat-2, Jason series 1–3, SARAL, and Sentinel 3. On average, we derive six estimates per year over the 28-year study period for each studied water body. We further provide a global-scale attribution of volume trends in natural lakes using a statistical-learning framework that incorporates major natural and anthropogenic drivers estimated from global climate data and hydrologic models. For reservoirs, we aggregate impacts of recent dam construction and subsequent reservoir infilling using newly compiled global dam and reservoir inventories (25), as well as sedimentation using in situ sediment surveys and upscaling methods. Finally, we isolate lake storage trends between arid and humid regions and quantify the numbers of local population subject to lake water losses.

Global LWS trends and drivers

We identify widespread decline in global LWS over the past 28 years. Over half ($53 \pm 2\%$) of the large lakes experienced significant water losses

¹Cooperative Institute for Research in Environmental Sciences (CIRES), University of Colorado Boulder, Boulder, CO 80309, USA. ²Department of Civil, Environmental and Architectural Engineering, University of Colorado Boulder, Boulder, CO 80309, USA. ³Department of Geography and Geospatial Sciences, Kansas State University, Manhattan, KS 66506, USA.

⁴Laboratoire d'Études en Géophysique et Océanographie Spatiales (LEGOS), Université de Toulouse, CNES-IRD-CNRS-UT3, Centre National d'Études Spatiales (CNES), 31013 Toulouse, France. ⁵Climate and Livability Initiative, Center for Desert Agriculture, Biological and Environmental Science and Engineering Division, King Abdullah University of Science and Technology, Thuwal 23955, Saudi Arabia. ⁶International Institute for Applied Systems Analysis (IIASA), A-2361 Laxenburg, Austria.

*Corresponding author. Email: fangfang.yao@colorado.edu; yaoff.luke@gmail.com

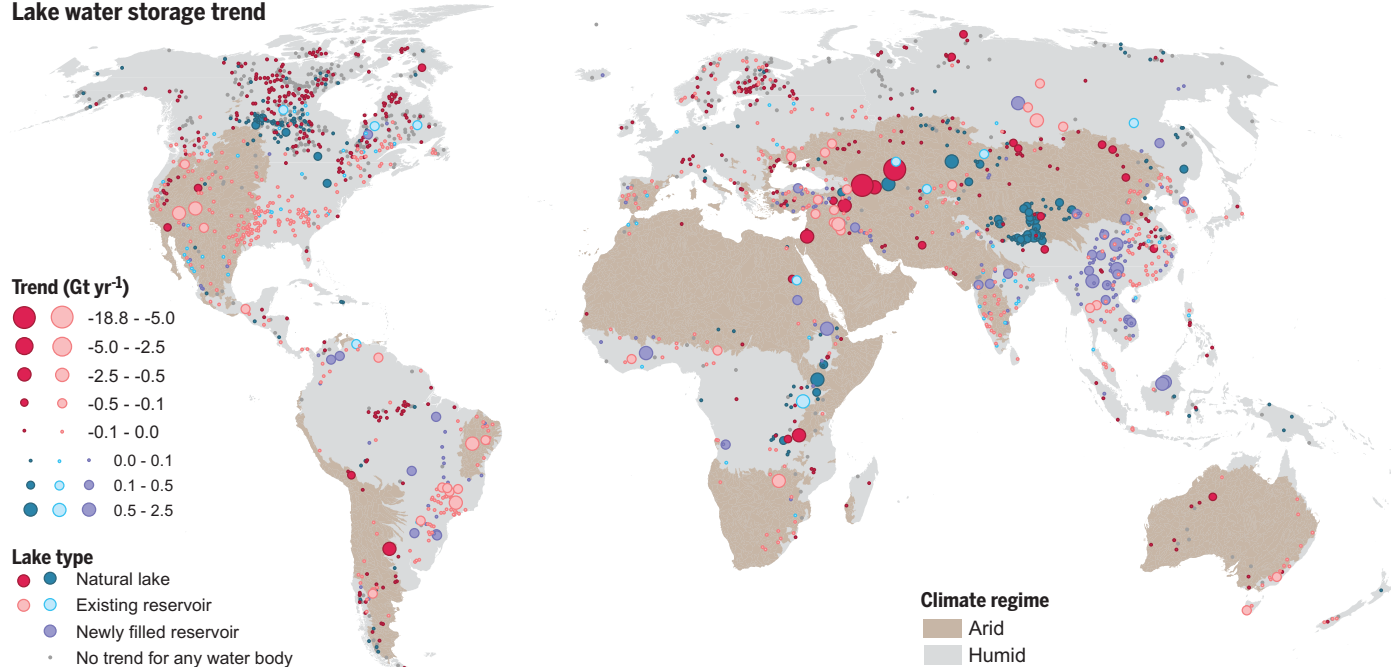
Lake water storage trend

Fig. 1. Widespread storage decline in large global lakes from October 1992 to September 2020. Lake water storage (LWS) trends for 1058 natural lakes (dark red and dark blue dots) and 922 reservoirs (light red and light blue dots). Recently filled reservoirs after 1992 are denoted as light purple dots. All colored

dots denote statistically significant trends ($p < 0.1$), whereas no significant trends are shown as gray dots. Classification of climate regimes between arid and humid regions was done using the aridity index [ratio of mean annual precipitation to mean annual potential evapotranspiration (materials and methods)].

($p < 0.1$) (Fig. 1). LWS loss prevails across major global regions including western Central Asia, the Middle East, western India, eastern China, northern and eastern Europe, Oceania, the continental United States, northern Canada, southern Africa, and most of South America. Roughly one-quarter (24%) of the large lakes experienced significant water gains, which are largely found in dam-construction hotbeds and in remote or underpopulated regions, such as the Inner Tibetan Plateau and the Northern Great Plains of North America. Globally, LWS showed a net decline at a rate of $-21.51 \pm 2.54 \text{ Gt year}^{-1}$ (Fig. 2, A and D), or by 602.28 km^3 in accumulative volume—equivalent to the total water use in the US for the entire year of 2015 or 17 times the volume of Lake Mead, the largest reservoir in the United States (Fig. 2, A and D). The accumulative volume loss in global LWS is about 40% larger than the mean of annual variations (i.e., differences between maximum and minimum values) in global LWS over the period 1992–2020, masking its importance to the water cycle and freshwater resources.

Globally, natural lake volume declined at a net rate of $-26.38 \pm 1.59 \text{ Gt year}^{-1}$, of which $56 \pm 9\%$ is attributable to direct human activities and changes in temperature and potential evapotranspiration (PET), i.e., evaporative demand (Fig. 2G). A total of 457 natural lakes (43%) had significant water losses with a total rate of $-38.08 \pm 1.12 \text{ Gt year}^{-1}$, whereas sig-

nificant water gains were found in 234 natural lakes (22%) at a total rate of $13.02 \pm 0.41 \text{ Gt year}^{-1}$. The remaining 360 lakes (35%) showed no significant trends (Fig. 1). Over 80% of the total decline in drying lakes stems from the 26 largest losses ($>0.1 \text{ Gt year}^{-1}$, $p < 0.1$) (Fig. 3A). In particular, the largest inland water body, the Caspian Sea, accounts for 49% of the total decline and 71% of the net decline in natural LWS (fig. S1). Unsustainable water consumption dominates the observed drying of the Aral Sea ($-6.59 \pm 0.36 \text{ Gt year}^{-1}$) in Central Asia, Lake Mar Chiquita ($-0.75 \pm 0.09 \text{ Gt year}^{-1}$) in Argentina, the Dead Sea ($-0.63 \pm 0.04 \text{ Gt year}^{-1}$) in the Middle East, and the Salton Sea ($-0.11 \pm 0.01 \text{ Gt year}^{-1}$) in California. Increasing temperature and PET led to the complete disappearance of Lake Good-e-Zarez ($-0.48 \pm 0.17 \text{ Gt year}^{-1}$) in Afghanistan, Toshka lakes ($-0.13 \pm 0.10 \text{ Gt year}^{-1}$) in Egypt, and marked drying of Lake Kara-Bogaz-Gol ($-1.27 \pm 0.09 \text{ Gt year}^{-1}$) in Turkmenistan, Lake Khyargas ($-0.35 \pm 0.03 \text{ Gt year}^{-1}$) in Mongolia, and Lake Zonag ($-0.26 \pm 0.14 \text{ Gt year}^{-1}$) in China. The remaining change is primarily attributable to changes in precipitation and runoff, including the Caspian Sea ($-18.80 \pm 0.93 \text{ Gt year}^{-1}$), Lake Urmia ($-1.05 \pm 0.06 \text{ Gt year}^{-1}$) in Iran, the Great Salt Lake ($-0.29 \pm 0.08 \text{ Gt year}^{-1}$) in the United States, Lake Poyang ($-0.13 \pm$

$0.12 \text{ Gt year}^{-1}$) in China, Lake Titicaca ($-0.12 \pm 0.08 \text{ Gt year}^{-1}$) on the border of Bolivia and Peru, and others, which largely agrees with existing studies (8, 12, 13, 26). Whereas a recent study suggests that the drying of Lake Urmia was primarily attributed to human activities (27), we find that naturalized flows explain 67% of the variance in the annual mean lake volume compared with 52% explained by human water consumption. Thus, the decline of Lake Urmia is likely a concurrent result of both reduced naturalized flows and human activities. Arctic lakes were mostly in decline owing to a combination of changes in precipitation, runoff, temperature, and PET (Fig. 3A), which are likely a concurrent result of natural variability and climate change. Globally, temperature-and-PET changes dominate water loss in 21% of the drying lakes (Fig. 3A). Approximately one-third of the total decline in all drying lakes is offset by lake storage increases elsewhere, largely in remote or sparsely populated areas such as the Inner Tibetan Plateau, Northern Great Plains, and Great Rift Valley (Fig. 3B). These storage increases were driven primarily by changes in precipitation and runoff, and to a lesser extent, by temperature-and-PET changes and reduced human water use. For example, Lake Sevan in Armenia experienced an increasing storage trend (0.20 ± 0.02) owing to the enforcement of conservation laws on water withdrawal since the 2000s (28).

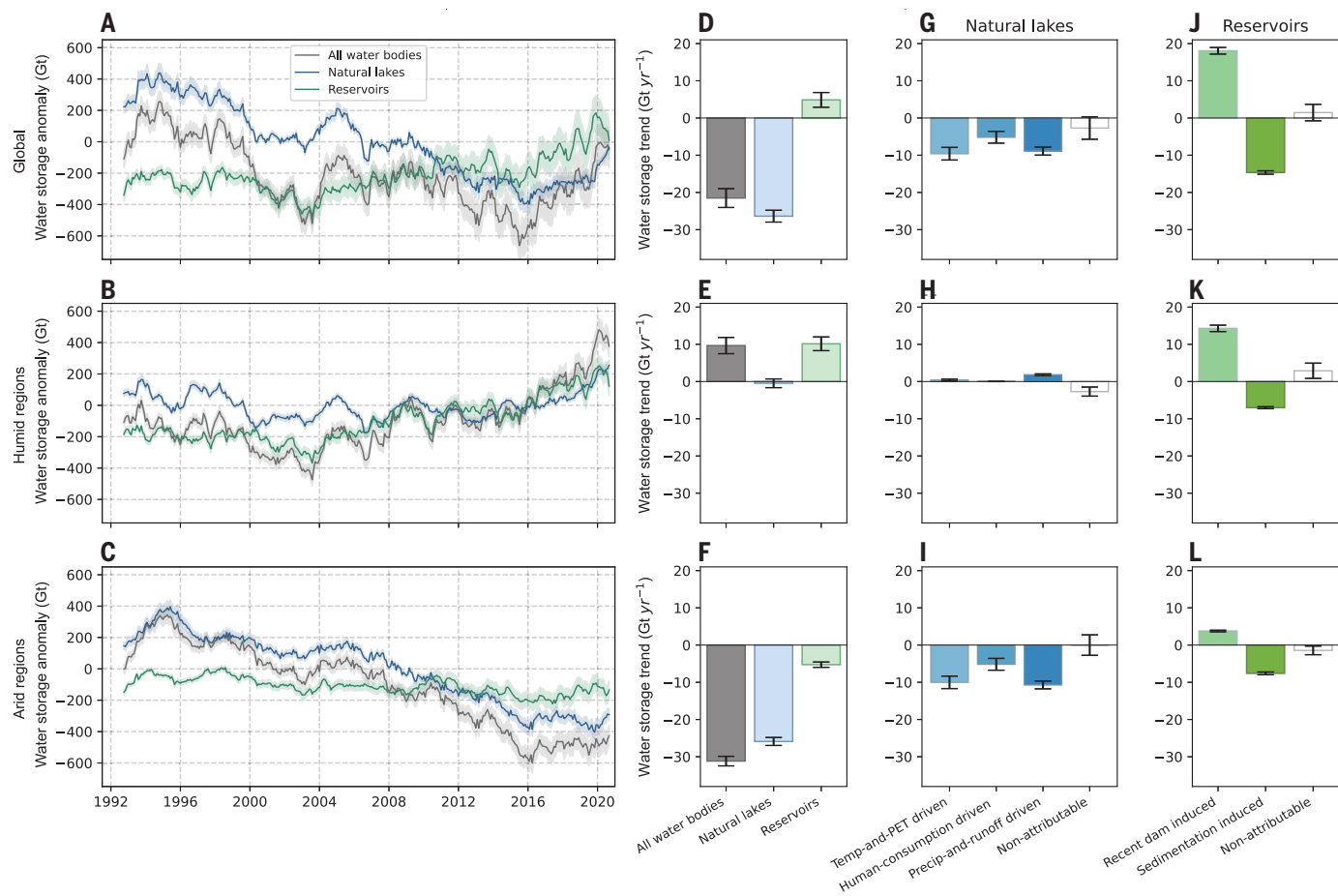


Fig. 2. Time series and drivers of global lake water storage change, October 1992 to September 2020. (A to F) Time series and trends of aggregate storage anomalies for each type of water body for global, humid, and arid regions, respectively. **(G to L)** Attribution of storage trends in natural lakes and reservoirs. Temp, Precip, and PET stand for temperature, precipitation, and potential evapotranspiration, respectively. The shading denotes the LWS uncertainties in all water bodies (gray shading), natural lakes (blue shading), and

reservoirs (green shading) at a 95% confidence interval. The error bars show the aggregate uncertainty in LWS trends at a 95% confidence interval. For natural lakes, 57% of the net global decline is attributable to human activities and increasing temperature and potential evapotranspiration. Recent dam construction, largely in humid basins, supported the net increase in global reservoir storage, although more than 80% of the increased storage in recently filled reservoirs is offset by sedimentation-induced storage loss in existing reservoirs.

Nearly two-thirds ($64 \pm 4\%$) of all large reservoirs experienced significant storage declines, although reservoirs showed a net global increase at a rate of $4.87 \pm 1.98 \text{ Gt year}^{-1}$, owing to 183 (20%) recently filled reservoirs. Storage declines in existing reservoirs, i.e., filled before 1992, were observed in most regions. Global storage decline in existing reservoirs ($-13.19 \pm 1.77 \text{ Gt year}^{-1}$) can be largely attributed to sedimentation (Fig. 2J), which is consistent with observations of substantial storage decline in US reservoirs due to sedimentation (29, 30). Globally, sedimentation-induced storage loss offsets more than 80% of the increased storage from new dam construction (Fig. 2J). Our finding suggests that sedimentation is the primary contributor to the global storage decline in existing reservoirs and has a larger impact than hydroclimate variability, i.e., droughts and recovery from droughts (19). Recent droughts may have contributed to re-

servoir storage declines, particularly in the southwestern United States (31), eastern and southern Brazil (32), the Middle East (33), southern India (34), eastern and southeastern Asia (35), eastern Oceania (36), and most of Europe (37). However, drought impacts on reservoir LWS have been partially offset by wetting trends elsewhere (12), such as the headwaters of the Nile River, southeastern Canada, and Mexico (Fig. 1).

LWS trends in arid and humid regions

Arid regions experienced a net storage decline for both natural lakes and reservoirs at a rate of -25.90 ± 1.07 and $-5.27 \pm 0.71 \text{ Gt year}^{-1}$, respectively. Approximately 60% of the water bodies in arid regions had significant water losses. More than 70% of the total LWS loss in these water bodies stemmed from 10 basins with either a drying climate or unsustainable human water consumption or both, such as in

the Aral Sea Basin and the Colorado River Basin (Fig. 4). The basins of the Caspian Sea, the Aral Sea, Lake Good-e-Zareh, Lake Urmia, Lake Rukwa, Lake Chiquita, the Dead Sea, and western Mongolia are large contributors to the global net decline in natural LWS. However, the vast majority (93%) of natural lakes with significant water losses are found in basins elsewhere and are distributed widely across the globe, which is in line with the widespread global decline in LWS seen in Fig. 1. In arid regions, roughly one-quarter of the significant water losses in natural lakes were dominated by changes in temperature and PET or human activities, and another 37% of the water losses were primarily attributable to reduced natural flows. Storage declined in more than two-thirds ($68 \pm 3\%$) of reservoirs in arid regions. The net reservoir storage loss was mostly attributable to sedimentation (Fig. 2L), although droughts likely aggravated reservoir storage losses, such

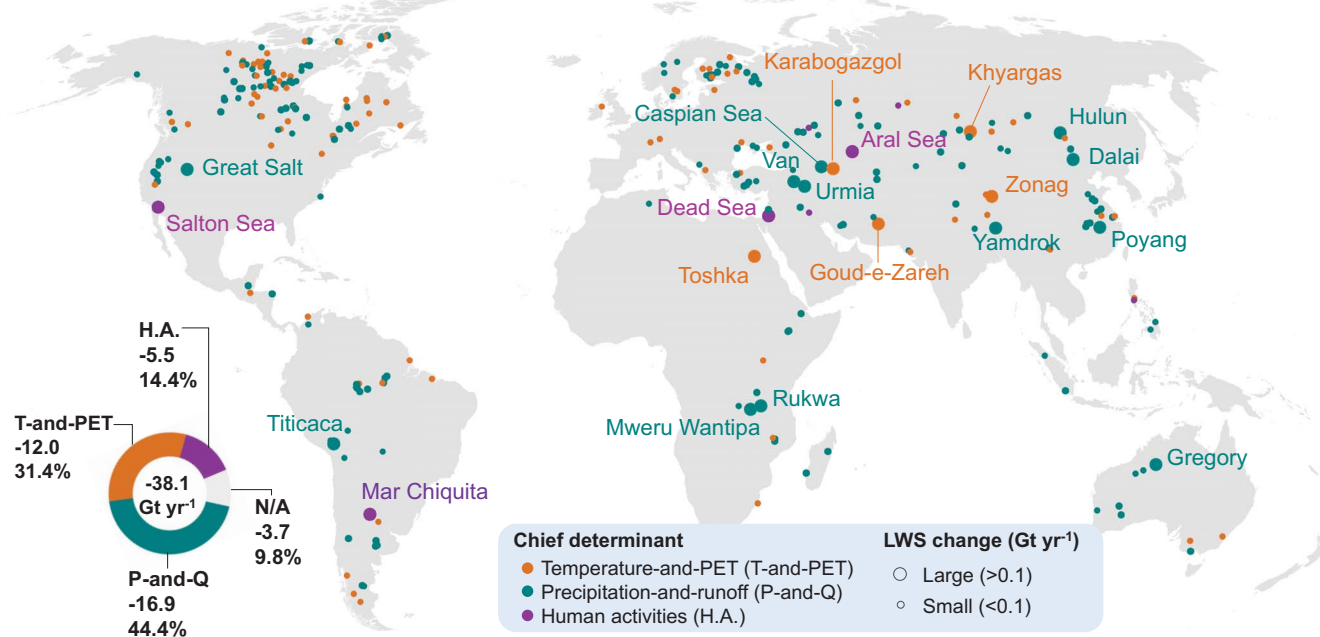
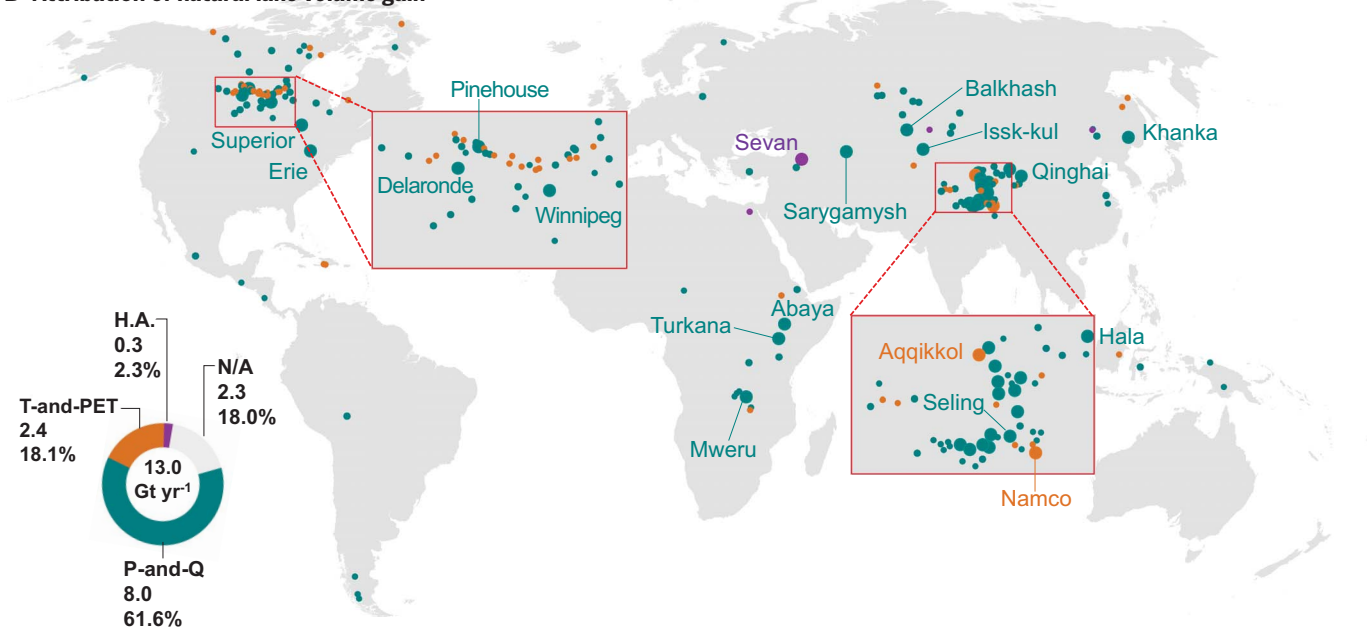
A Attribution of natural lake volume loss**B Attribution of natural lake volume gain**

Fig. 3. Attributions of significant volume changes in natural lakes. (A) Chief determinants for volume losses. (B) Chief determinants for volume gains. PET, potential evapotranspiration. The inset pie charts show the aggregate impact (by magnitude) of each determinant on the basis of relative contributions. For clarity, lake volume changes that are not significantly attributable (N/A) are not shown in panels (A) and (B), but their proportions are included in the insets.

as in the Colorado River Basin and the Tigris and Euphrates Basin (33, 38). Newly filled reservoirs resulted in a total of $3.77 \pm 0.21 \text{ Gt year}^{-1}$ of water gain, which partially offsets the net decline in reservoir storage by 42%. These new reservoirs are mainly found in the Nile, Volta, Yellow, and Amur River Basins. In the Nile Basin, newly filled reservoirs account for 41% of the increased basin water storage, and the remain-

ing 61% was largely attributable to the rapid rise of the regulated Lake Victoria in the headwater of the White Nile under precipitation extremes in 2019–2020 (39). A few other arid basins, such as the Inner Tibetan Plateau, Lake Balkhash, Great Rift Valley, and basins, experienced major water gains due to recovery from droughts and increasing precipitation (8, 12, 40) (Fig. 3).

New construction of reservoirs drove a net LWS gain in humid regions at a rate of $9.66 \pm 2.19 \text{ Gt year}^{-1}$, although 54% of the remaining water bodies showed significant storage declines. A total of 124 newly filled reservoirs in humid regions gained storage at a rate of $14.28 \pm 0.86 \text{ Gt year}^{-1}$, which offsets the total storage decline in existing reservoirs ($-4.15 \pm 1.63 \text{ Gt year}^{-1}$). Globally, more than 85% of

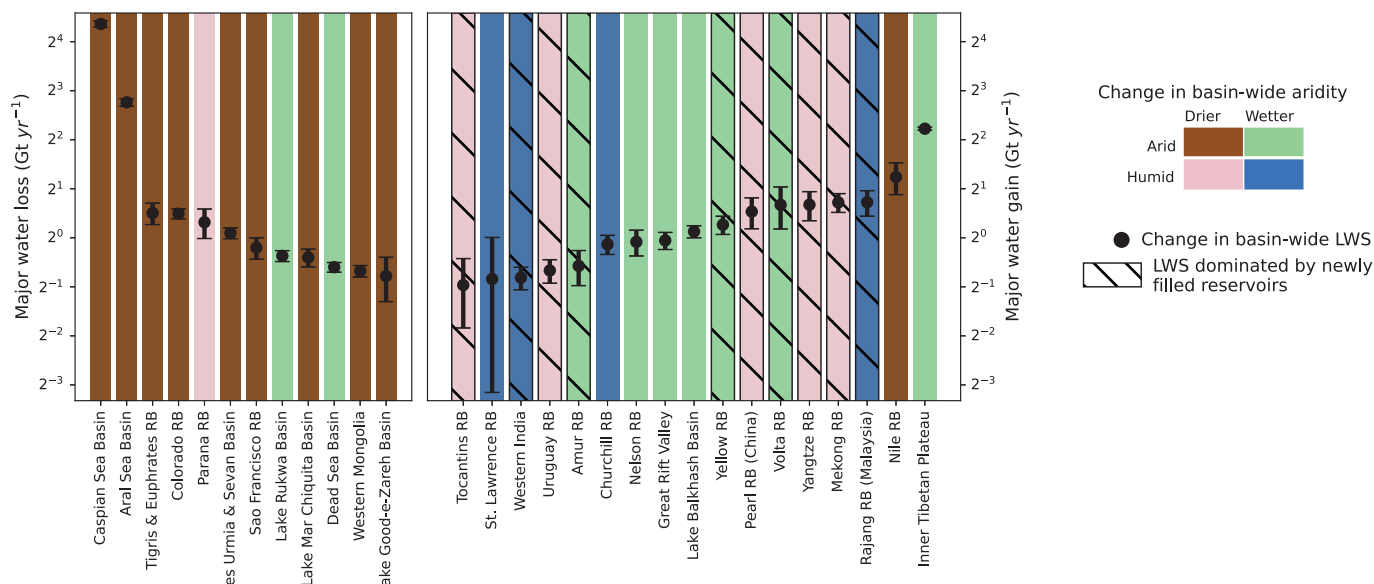


Fig. 4. Major losses and gains greater than 0.5 Gt year⁻¹ in basin-wide lake water storage. Bar colors represent the trending direction in aridity in arid and humid basins. The hatched area indicates basins where the LWS trend was dominated by recently filled reservoirs. The error bars

show the aggregate uncertainty in LWS trends at a 95% confidence interval. RB, for river basin. Major losses are primarily found in arid basins that are getting drier, and major gains in humid basins are mostly due to recent reservoir filling.

the newly filled reservoirs are concentrated in a few basins experiencing a dam construction boom, including the Nile, Yangtze, Mekong, Volta, Rajang, Pearl, Yellow, Amur, Uruguay, and Tocantins basins, as well as in western India (Fig. 4). About 55% of these regions experienced a drying climate during the study period, suggesting that human activities partially reversed the negative impact of climate on basin-wide surface water storage by impounding more water in reservoirs. Beyond these dam-construction hotbeds, most (65%) reservoirs experienced significant storage declines in humid regions (Fig. 1), indicating that the benefits of increased new reservoir storage are not evenly distributed. Most natural lakes were also in decline in humid regions, including high latitudes and the tropics (Fig. 1). However, these natural lake-volume losses were offset by precipitation-and-runoff-driven LWS gains in the northern Great Plains and the Laurentian Great Lakes of North America (Fig. 3B).

Discussion

We leveraged three decades of satellite observations to map long-term global LWS variability, finding evidence of widespread decline in global LWS with more than half of large water bodies ($53 \pm 2\%$) exhibiting significant drying trends. Roughly, one-quarter of the significant water losses in natural lakes were dominated by human activities or increasing temperature and PET, with the latter changes most often attributed to climate change (41, 42). Before

this study, many of the human and climate change footprints were either unknown, such as the desiccations of Lake Good-e-Zareh in Afghanistan and Lake Mar Chiquita in Argentina, or known only anecdotally, as in northern Eurasia and Canada. These water losses affect both the water and carbon cycles. For example, Arctic lakes are drying partially because of changes in temperature and PET (Fig. 3A), which is in line with broader climate changes toward increasing evaporative loss due to higher lake temperatures and reduced lake ice extents (43–45). Changes in runoff could also contain a climate change footprint through increasing evaporation (46, 47). If we assume that some fraction of runoff-driven water losses are attributable to climate change, 43% of drying lakes were at least partially influenced by climate change as water losses were dominated by changes in temperature, PET, or runoff (fig. S2). Widespread LWS decline, particularly accompanied by rising lake temperatures, could reduce the amount of absorbed carbon dioxide and increase carbon emissions to the atmosphere given that lakes are hotspots of carbon cycling (3, 48). Alternatively, climate change can increase LWS, particularly in the Tibetan Plateau, where glacier retreat and permafrost thawing partially drove alpine lake expansion (8, 40), and in regions where precipitation is projected to increase under warming, such as the Upper Mississippi River Basin (49).

Our findings suggest that drying trends worldwide are more extensive than previously thought

(8, 12, 21). Luo *et al.* (21) reported a net global increase in natural lake storage at a rate of $16.12 \text{ Gt year}^{-1}$ and that most of the global lakes in humid regions gained water storage, whereas lakes in arid regions with high human water stress were generally in decline over 2003–2020. Although we confirm a “dry-get-drier” pattern in LWS, our findings also show widespread LWS decline in the humid tropics and high-latitude regions over the past three decades, as well as a net global decline ($-26.38 \pm 1.59 \text{ Gt year}^{-1}$) in natural lake storage. This contrast indicates that extrapolating the trends inferred from a brief time series could be uncertain, suggesting the necessity for long-term observations. For example, Luo *et al.* (21) concluded that Amazon lakes are largely expanding on the basis of LWS time series over two short periods (2003–2009 and 2018–2020). By contrast, the vast majority of large Amazon lakes in our study show a decreasing LWS trend because our detailed multidecadal LWS time series fully capture the impacts of major droughts during the early 2000s, 2010, and 2015. More broadly, our finding indicates that an intensified water cycle in a warming climate (50) may not result in increased water storage in humid regions, in part because of increasing land evapotranspiration (51) and potentially longer drought recovery times (52). The continued observations from ongoing and new satellites, in particular the Surface Water and Ocean Topography (SWOT) mission (recently launched in December 2022), will be useful to

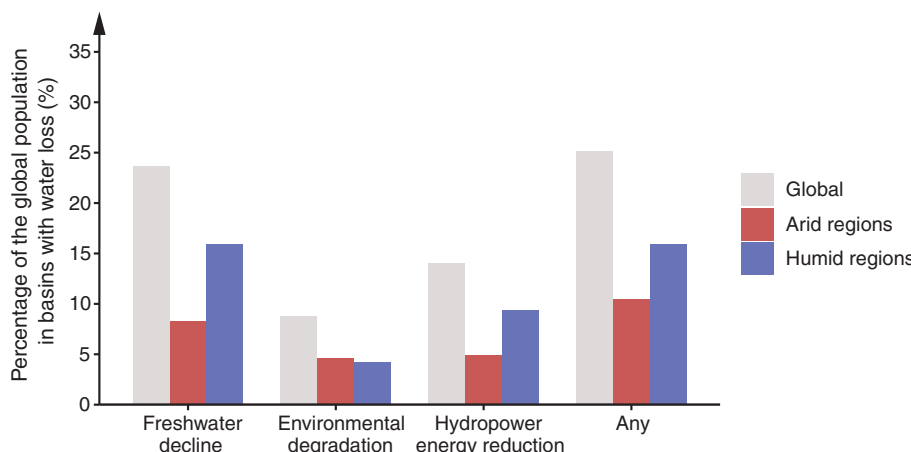


Fig. 5. Percentages of the global population residing in basins experiencing significant lake water

loss. Affected sectors associated with lake water loss are freshwater decline, environmental degradation, and hydropower energy reduction. Approximately one-quarter of the global population resides in basins with lake water loss, partitioned comparably between arid and humid regions.

extend the LWS trends observed here and enable longer-term assessments of the interactions among LWS, the water cycle, and climate change.

This global-scale attribution of LWS trends has important implications for water resources management, particularly given that up to 2.0 billion people (one-quarter of the global population in 2023) reside in basins with large water bodies experiencing significant water storage losses (Fig. 5). Many of these drying lakes have been identified as important sources of water and energy (hydropower) (22) or listed among Ramsar sites of international importance (53). About 24, 9, and 14% of the global population resides in basins that are experiencing freshwater decline, environmental degradation, and hydropower energy reduction associated with decreasing LWS, respectively (Fig. 5). These population numbers can be roughly divided between arid and humid regions, with the latter having slightly larger shares. The reported populations are only estimates of potential impacts on lake basin residents who are likely the most affected by lake water loss (4, 54). Sedimentation dominates the water loss in existing reservoirs, which suggests that reservoirs on which populations are heavily reliant will become less reliable for freshwater and hydroelectric energy supply because of aging. Sedimentation-induced storage water losses need to be considered in sustainable future freshwater supplies and long-term planning for reservoir operations and construction of new dams (29). More than half of the net loss in natural lake volume ($56 \pm 9\%$) is attributable to human activities and increasing temperature and PET, indicating that any recovery of water storage in these lakes could require substantial management efforts. Our findings are broadly

consistent with existing studies (7, 27, 55) on human footprints on the Aral Sea, Dead Sea, and Lake Urmia but also reveal additional undocumented human-driven LWS losses in other large lakes, such as the Salton Sea in California and Lake Mar Chiquita in Argentina. The strongest attribution of human activities to LWS losses generally occurred in closed basins that were getting drier. This suggests that under conditions of declining precipitation, more-intensive human-water withdrawal from rivers led at least partially to the desiccations of closed lakes. Effective water conservation efforts can help save these water bodies (4), as shown in the success of recovering Lake Sevan through enacting water protection laws in Armenia (28). We detect that increasing temperature and PET are the chief determinants of water loss in 21% of drying natural lakes, a cautionary finding for a projected warmer future, underscoring the importance of accounting for climate change impacts within future surface water resources management.

REFERENCES AND NOTES

- M. L. Messager, B. Lehner, G. Grill, I. Nedeva, O. Schmitt, *Nat. Commun.* **7**, 13603 (2016).
- G. E. Hutchinson, *A Treatise on Limnology* (Wiley, ed. 1, 1957).
- C. E. Williamson, J. E. Saros, W. F. Vincent, J. P. Smol, *Limnol. Oceanogr.* **54**, 2273–2282 (2009).
- W. A. Wurtsbaugh et al., *Nat. Geosci.* **10**, 816–821 (2017).
- P. H. Gleick, *Int. Secur.* **18**, 79–112 (1993).
- A. D. Gronewold, C. A. Stow, *Science* **343**, 1084–1085 (2014).
- J.-F. Cretaux, R. Letolle, M. Bergé-Nguyen, *Global Planet. Change* **110**, 99–113 (2013).
- J. Wang et al., *Nat. Geosci.* **11**, 926–932 (2018).
- L. Feng, C. Hu, X. Chen, X. Zhao, *Environ. Sci. Technol.* **47**, 9628–9634 (2013).
- J.-F. Cretaux et al., *Surv. Geophys.* **37**, 269–305 (2016).
- J. L. Chen et al., *Geophys. Res. Lett.* **44**, 6993–7001 (2017).
- M. Rodell et al., *Nature* **557**, 651–659 (2018).
- J. Wang, Y. Sheng, Y. Wada, *Water Resour. Res.* **53**, 3854–3877 (2017).
- J.-F. Pekel, A. Cottam, N. Gorelick, A. S. Belward, *Nature* **540**, 418–422 (2016).
- Y. Wada et al., *Hydrol. Earth Syst. Sci.* **21**, 4169–4193 (2017).
- D. Tokuda, H. Kim, D. Yamazaki, T. Oki, *Geosci. Model Dev.* **14**, 5669–5693 (2021).
- C. Schwatke, D. Dettmering, W. Bosch, F. Seitz, *Hydrol. Earth Syst. Sci.* **19**, 4345–4364 (2015).
- T. Busker et al., *Hydrol. Earth Syst. Sci.* **23**, 669–690 (2019).
- H. Gao, C. Birkett, D. P. Lettenmaier, *Water Resour. Res.* **48**, W09504 (2012).
- S. W. Cooley, J. C. Ryan, L. C. Smith, *Nature* **591**, 78–81 (2021).
- S. Luo et al., *Geophys. Res. Lett.* **49**, 1–10 (2022).
- B. Lehner et al., *Front. Ecol. Environ.* **9**, 494–502 (2011).
- M. M. Tilzer, C. Serruya, *Large Lakes* (Springer Berlin Heidelberg, Berlin, Heidelberg, 1990).
- F. Yao, J. Wang, C. Wang, J.-F. Cretaux, *Remote Sens. Environ.* **232**, 111210 (2019).
- J. Wang et al., *Earth Syst. Data* **14**, 1869–1899 (2022).
- Y. Moon, U. Lall, H. Kwon, *Int. J. Climatol.* **28**, 361–370 (2007).
- S. Chaudhari, F. Felfani, S. Shin, Y. Pokhrel, *J. Hydrol. (Amst.)* **560**, 342–353 (2018).
- A. Medvedev et al., *Remote Sens. (Basel)* **12**, 3821 (2020).
- T. J. Randle et al., *J. Hydrol. (Amst.)* **602**, 126686 (2021).
- W. L. Graf, E. Wohl, T. Sinha, J. L. Sabo, *Water Resour. Res.* **46**, W12535 (2010).
- A. P. Williams et al., *Science* **368**, 314–318 (2020).
- A. Getirana, *J. Hydrometeorol.* **17**, 591–599 (2016).
- N. Chao, Z. Luo, Z. Wang, T. Jin, *Ground Water* **56**, 770–782 (2018).
- V. Mishra, K. Thirumalai, S. Jain, S. Aadhar, *Environ. Res. Lett.* **16**, 054007 (2021).
- M. Venkatappa, N. Sasaki, P. Han, I. Abe, *Sci. Total Environ.* **795**, 148829 (2021).
- A. I. J. M. van Dijk et al., *Water Resour. Res.* **49**, 1040–1057 (2013).
- T. A. Brás, J. Seixas, N. Carvalhais, J. Jägermeyr, *Environ. Res. Lett.* **16**, 065012 (2021).
- M. Xiao, B. Udall, D. P. Lettenmaier, *Water Resour. Res.* **54**, 6739–6756 (2018).
- M. Khaki, J. Awange, *Sensors* **21**, 4304 (2021).
- F. Yao et al., *Environ. Res. Lett.* **13**, 064011 (2018).
- R. A. Kerr, *Science* **316**, 188–190 (2007).
- D. G. Kingston, M. C. Todd, R. G. Taylor, J. R. Thompson, N. W. Arnell, *Geophys. Res. Lett.* **36**, L20403 (2009).
- C. M. O'Reilly et al., *Geophys. Res. Lett.* **42**, 10773–10781 (2015).
- S. Sharma et al., *Nat. Clim. Chang.* **9**, 227–231 (2019).
- G. Zhao, Y. Li, L. Zhou, H. Gao, *Nat. Commun.* **13**, 3686 (2022).
- N. S. Christensen, A. W. Wood, N. Voisin, D. P. Lettenmaier, R. N. Palmer, *Clim. Change* **62**, 337–363 (2004).
- J. R. Miller, G. L. Russell, *J. Geophys. Res.* **97** (D3), 2757 (1992).
- J. A. Rosentreter et al., *Nat. Geosci.* **14**, 225–230 (2021).
- E. Sinha, A. M. Michalak, V. Balaji, *Science* **357**, 405–408 (2017).
- M. R. Allen, W. J. Ingram, *Nature* **419**, 224–232 (2002).
- D. G. Miralles et al., *Nat. Clim. Chang.* **4**, 122–126 (2014).
- C. R. Schwalm et al., *Nature* **548**, 202–205 (2017).
- Ramsar Sites Information Service (Ramsar, accessed 24 November 2021); <https://rslis.ramsar.org/>.
- W. S. Breffle et al., *Resour. Policy* **38**, 152–161 (2013).
- R. A. Al-Weshah, *Hydrol. Process.* **14**, 145–154 (2000).

ACKNOWLEDGMENTS

We thank A. Temme, C. Martin, S. Nerem, and J. Rosentreter for comments on the results and K. Yang and K. Bogan for suggestions and assistance on the visualizations. We thank P. Lin for sharing the latest version of the GRADES data and H. Beck for sharing the latest version of the MSWEP data for our analyses. Assistance for processing climate and human water use datasets was provided by K. Yang. We also thank L. Patterson for help with downloading the in situ data of reservoirs and L. Pitcher and E. Knight for proofreading our manuscript. We thank C. Schwatke, C. Birkett, and S. Cooley for making the altimetry-derived water level data publicly available. **Funding:** This study was supported by NOAA Cooperative Agreement with Cires (NA17OAR4320101) to F.Y., NASA NIP grant (80NSSC18K0951) to B.L., and the “Climate Change Initiative Grant (4000125030/181/NB) to J.-F.C. and M.B.-N.” **Author contributions:** F.Y. conceptualized the project. F.Y., J.W., J.-F.C., and M.B.-N. estimated and analyzed

the water storage variability and trends. F.Y., B.R., and B.L. developed the statistical models. F.Y. and B.R. estimated the sedimentation-induced storage loss in reservoirs. F.Y. evaluated the potential impacts of drying lakes on population with inputs from B.L., B.R., and Y.W. F.Y. conducted the validation. F.Y. performed the visualization with inputs from B.L., J.W., and Y.W. F.Y. wrote the manuscript with inputs from B.L., B.R., and J.W. All authors read and commented on drafts of this paper.

Competing interests: The authors declare no competing interests.
Data and materials availability: The Landsat images, including Landsat 5 Thematic Mapper, Landsat 7 Enhanced Thematic Mapper-plus, and Landsat 8 Operational Land Imager, are available from the US Geological Survey at <http://earthexplorer.usgs.gov> and the Google Earth Engine platform at <https://earthengine.google.com>. ICESat and ICESat-2 data are available from the National Snow and Ice Data Center (NSIDC) at <https://nsidc.org/data>. Water levels derived from ICESat-2 are available at <https://doi.org/10.5281/zenodo.4489056>. Water level products from radar altimeters can be downloaded from the Hydroweb at <http://hydroweb.theia-land.fr>, the Database for Hydrological Time Series of Inland Waters (DAHITI) at <https://dahiti.dgfi.tum.de/en>, and the USDA Global Reservoir and Lake Monitor database at https://ipad.fas.usda.gov/cropexplorer/global_reservoir. The CryoSat-2 data are available from the European Space Agency (ESA) at <https://earth.esa.int/eogateway/catalog/cryosat-products>. The Global Reservoir Bathymetry Dataset can be downloaded from <https://dataVERSE.tdl.org/dataset.xhtml?persistentId=doi:10.18738/T8/T05HGJG>. The Global Surface Water (GSW) dataset is available from <https://global-surface-water.appspot.com/> and the Google Earth Engine platform at <https://earthengine.google.com>. Reservoir sedimentation survey data from the US Army Corps can be accessed at <https://water.usace.army.mil/> and <https://nicholasinstitute.duke.edu/reservoir-national-trends/sediment/>. USGS gauge data can be downloaded from

<https://waterdata.usgs.gov/nwis/>, US Army Corps gauge data can be downloaded from <https://water.usace.army.mil/> and <https://nicholasinstitute.duke.edu/reservoir-data/>, California Department of Water Resources gauge data can be downloaded from <https://cdce.wat.ca.gov/>, gauge data from Texas Water Development Board can be downloaded from <https://waterdatafortexas.org/reservoirs/statewide>, gauge data from Spain can be downloaded from <https://ceh.cedex.es/anuarioafos/af0/embalse-nombre.asp>, and gauge data from Bureau of Meteorology in Australia can be downloaded from <http://www.bom.gov.au/waterdata/>. The HydrolAKES database can be downloaded from <https://www.hydrosheads.org/page/hydrolakes>. The Georeferenced global Dams And Reservoir dataset (GeoDAR) can be downloaded from <https://dol.org/10.5281/zenodo.6163413>. The database of Roller-Compacted Concrete (RCC) dams can be accessed at <http://www.rccdams.co.uk/>. The Global Lake area, Climate, and Population (GLCP) dataset can be downloaded at <https://portal.edirepository.org/nis/mapbrowse?packageid=edi.394.4>. The HydroSHEDS dataset can be downloaded from <https://hydrosheads.org/page/overview>. The Climatic Research Unit (CRU) data are available from <https://crudata.uea.ac.uk/cru/data/hr/g/>. ECMWF Reanalysis v5 (ERA5) data are available from <https://www.ecmwf.int/en/forecasts/datasets/reanalysis-datasets/era5>. Modern-Era Retrospective analysis for Research and Applications version 2 (MERRA-2) are available from <https://gmao.gsfc.nasa.gov/reanalysis/MERRA-2/>. Multi-Source Weighted-Ensemble Precipitation (MSWEP) are available from <https://www.gloh2o.org/mswep/>. Global Historical Climatology Network data are available from <https://www.ncdc.noaa.gov/products/land-based-station/global-historical-climatology-network-monthly>. Global Land Evaporation Amsterdam Model (GLEAM) data are available from <https://www.gleam.eu/>. Global Reach-scale A priori Discharge Estimates for SWOT (GRADES) dataset can be downloaded from <https://www.reachhydro.org/home/records/grades>. The

reconstructed human water use data derived from four global hydrologic models can be downloaded from <https://zenodo.org/record/1209296#YZPcr2DMKM8>. The water body masks delineated from the GSW dataset, lake volume time series derived from Landsat images and satellite altimeters, lake volume trend estimates, attribution, and all validation analyses are available on the Zenodo data repository at <https://zenodo.org/record/7946043>. Water storage trends and drivers of studied large lakes are available in the interactive map at <https://cires.colorado.edu/globallakes>.

Code availability: R scripts that were used to process hydroclimate and human water use data, to derive water levels from ICESat and ICESat-2, to construct lake water storage time series, to estimate the mean rate of sedimentation in reservoirs, to estimate trends in lake water storage and basin aridity, to conduct validation, to construct regression model ensemble, and to estimate affected population are available on CodeOcean at <https://codeocean.com/capsule/0322198/tree/v1>. JavaScript scripts for mapping water areas from Landsat images and IDL Scripts for processing CyoSat-2 data are available in the supplementary materials. **License information:** Copyright © 2023 the authors, some rights reserved; exclusive licensee American Association for the Advancement of Science. No claim to original US government works. <https://www.sciencemag.org/about/science-licenses-journal-article-reuse>

SUPPLEMENTARY MATERIALS

science.org/doi/10.1126/science.abo2812
 Materials and Methods
 Figs. S1 to S11
 References (56–100)

Submitted 11 March 2022; accepted 31 March 2023
 10.1126/science.abo2812